Available online at www.sciencedirect.com
ScienceDirect
International Journal of Mass Spectrometry 255–256 (2006) 93–101
International Journal of Mass Spectrometry
www.elsevier.com/locate/ijms

Competing rearrangement reactions in small gas-phase ionic complexes: The internal S_N2 and nitro-nitrite rearrangements in nitroalkane proton-bound pairs

Clement Poon, Paul M. Mayer *

Department of Chemistry, University of Ottawa, 10 Marie-Curie, Ottawa, Ont., K1N 6N5 Canada

Received 30 September 2005; received in revised form 24 January 2006; accepted 26 January 2006
Available online 20 March 2006

Dedicated to Diethard Böhme for his outstanding contributions to ion chemistry.

Abstract

The dissociation of metastable proton-bound pairs, $(R_1NO_2)(R_2NO_2)H^+$ (R_1 and $R_2 = CH_3$, CH_3CH_2, $(CH_3)_2CH$ and $(CH_3)_3C$) have been investigated by mass spectrometry and density functional theory calculations. The proton-bound pairs can dissociate via hydrogen-bond cleavage into protonated and neutral nitroalkanes. Methyl substitution of the nitroalkanes (R_1 and $R_2 = (CH_3)_2CH$, $(CH_3)_3C$) permits a rearrangement process to compete with the H-bond cleavage on the microsecond timescale. The rearrangement reaction results in an isomer that then loses nitrous acid and involves an internal S_N2-type mechanism in which $(R_1NO_2)(R_2NO_2)H^+$ isomerizes to $R_1NO_2\cdots R_2NO_2H^+$ via TS1 and then subsequently to $R_1NO_2R_2^+\cdots HONO$ via TS2 prior to dissociation. The process is favoured by stabilization of the charge in TS2 by methyl substitution. The stability of the *t*-butyl ion changes the mechanism in $((CH_3)_3CNO_2)_2H^+$ to one that involves a two-step alkyl cation transfer. An investigation of nitro-nitrite rearrangement in protonated nitroalkanes at the B3-LYP/6-31 + G(d) level of theory found that the rearrangement barrier is lowered to the point that $(CH_3)_3CNO_2H^+$ can easily interconvert into $(CH_3)_3CO(H)NO^+$ in the gas phase and leads to the conclusion that the proton-bound pairs involving $(CH_3)_3CNO_2$ are a mixture of nitro-nitro and nitro-nitrite proton-bound pairs. The nitrite isomer can dissociate into protonated *t*-butyl nitrite and neutral nitroalkane via a simple hydrogen-bond cleavage. A more favourable competing dissociation process leads to the loss of *t*-butanol to form the $((CH_3)_3CNO_2)(NO)^+$ complex.

Keywords: Nitroalkane; S_N2; Nitro-nitrite; Rearrangement; Proton-bound pairs

1. Introduction

A central feature of the chemistry of gaseous ions is their tendency to rearrange prior to dissociation when thermodynamically more stable and kinetically accessible isomers are present on the potential energy surface. Electrostatically bound ions such as proton-bound pairs undergo extensive rearrangement reactions. Proton-bound pairs of alcohols $(ROH)(R'OH)H^+$ exhibit an almost universal tendency to lose H_2O [1–5]. Calculations [6–11] and experiments [12–16] on the methanol proton-bound dimer indicated that isomerization proceeds via an internal S_N2-type reaction. Work from our laboratory and that of other labs also showed that the family of methyl-substituted nitrile-alcohol proton-bound pairs [9,11,17–20] and dimethyl ether proton-bound dimer [21] loses water and methanol in a similar fashion.

In this paper, we examine the tendency for proton-bound pairs involving nitroalkanes to lose nitrous acid. The potential energy surface for the proton-bound pairs and the effect of methyl substitution on the reaction barriers will be described. In the course of this investigation another rearrangement reaction was observed for certain proton-bound pairs involving 2-methyl-2-nitropropane, $(CH_3)_3CNO_2$. The 2-methyl-2-nitropropane proton-bound dimer loses a molecule of *t*-butanol in a process that involves the isomerization of $(CH_3)_3CNO_2H^+$ to $(CH_3)_3CO(H)NO^+$. Thermal decomposition of nitromethane has been extensively studied in the literature [22–29]. Theoretical and experimental studies are divided as to whether isomerization to methyl nitrite is competitive with dissociation to CH_3 and NO_2. An IRMPD study of methyl, ethyl and

* Corresponding author. Tel.: +1 613 562 5800 ext. 6038; fax: +1 613 562 5170.
E-mail address: pmmayer@uottawa.ca (P.M. Mayer).

1387-3806/$ – see front matter © 2006 Elsevier B.V. All rights reserved.
doi:10.1016/j.ijms.2006.01.036

isopropyl-substituted NO_2 showed evidence for the isomerization to methyl nitrite along with dissociation of nitromethane to $CH_3 + NO_2$, but no evidence for the isomerization of the other two nitroalkanes [22]. In contrast, the rearrangement barrier is significantly lowered in nitrosilane [30]. A more recent study on nitroalkane molecules and their radical cations [31] showed that while the reaction fails to occur at room temperature with most aliphatic nitroalkanes, the barrier is greatly reduced in the corresponding radical cations. The effect on the barrier is often explained in terms of electronegativity [30] or atomic charges [31] but contention exists about the nature of the transition state in the isomerization mechanism. If the C–N bond is completely broken before the C–O bond begins to form (a loose transition state), the reaction can be described as the interaction of two radical fragments, $CH_3NO_2 \rightarrow CH_3 + NO_2 \rightarrow CH_3ONO$. In contrast, if the bond cleavage is not complete, a tighter transition state results and the reaction is described as $CH_3NO_2 \rightarrow CH_3ONO$. Dewar et al. [24] and McKee [25] found a tight transition state for the nitro-nitrite rearrangement of CH_3NO_2 with MINDO/3 and HF/6-31G* calculations, respectively. McKee, however, anticipated that the method would poorly describe the unimolecular transition state since they are based on a single-determinant wave function while the transition state is expected to have considerable open-shell character. When calculated at 4X4CAS-MCSCF/6-31G* level of theory, the C–N and C–O bonds of the transition state lengthen to about 3.396 and 3.654 Å, respectively [26]. Such a loose transition state was also obtained by Saxon and Yoshimine at the MCSCF/4-31G level of theory with 7 orbital active space [27]. DFT and CASPT2 study by Arenas et al. [29], on the other hand, confirms a tight transition state. He concluded that the loose transition states seem to be artifacts, either due to the very small active space used or the symmetry breaking effect which is present in the calculation. To the best of our knowledge, no nitro-nitrite rearrangement has been reported for proton-bound pairs. In this paper, we will look into the effect of proton attachment on the nitro-nitrite rearrangement barrier in nitroalkanes and how it relates to the unimolecular chemistry of nitroalkane proton-bound pairs.

2. Experimental and computational procedures

All experiments were performed on a modified VG ZAB mass spectrometer [32], incorporating a magnetic sector followed by two electrostatic sectors (BEE geometry) (VG Analytical, Manchester, UK). Protonated cluster ions were generated in a high-pressure ion source of the instrument [33]. The pressures in the ion source chamber, monitored with an ionization gauge located above the ion source diffusion pump, were typically between 10^{-5} and 10^{-4} mbar (the pressure in the ion source itself being approximately three orders of magnitude higher). Cluster ions were not observed when the pressure was below 10^{-6} mbar, and there was no evidence of higher order clusters at any of the pressures used in these experiments. The ion accelerating voltage was 8 kV except for source-generated $((CH_3)_2CHNO_2)(NO)^+$ and $((CH_3)_3CNO_2)(NO)^+$ ions which were accelerated by 5 kV to give them a similar energy to the metastably generated product ions from their parent proton-bound pairs. Metastable ion (MI), collision-induced dissociation (CID) and neutralization–reionization (NR) mass spectra were recorded in the usual manner in the second and third field-free region of the instrument [34]. Helium collision gas was used in all CID experiments and was introduced into the collision cells to achieve a 10% reduction in the ion flux (i.e., single collision conditions). For the NR experiments, oxygen gas was introduced to both collision cells for neutralization and reionization such that each cell achieves a 10% reduction in the ion flux and a potential of +500 V was applied to a deflector electrode located between the two cells. All spectra were recorded with the ZAB-CAT program developed by Mommers Technologies [35]. All chemicals were commercially obtained and used without further purification. Isotopically labelled compounds (C/D/N Isotopes Ltd, Montreal, QC, Canada) were of over 99% purity.

Standard ab initio molecular orbital calculations [36] were performed using the Gaussian 98 suite of programs [37]. Optimized geometries and the energies of all minima and transition states were calculated at the B3-LYP/6-31 + G(d) level of theory. Zero-point energies were scaled by a factor of 0.9806 as recommended by Scott and Radom [38]. Transition states were confirmed by the intrinsic reaction coordinate procedure in GAUSSIAN 98. The potential energy profile for the rearrangement of the nitromethane dimer was also obtained at the MP2/6-31 + G(d) and G3 (on B3-LYP geometries) [39] levels of theory for comparison to the B3-LYP/6-31 + G(d) results.

The nitrite form of the proton-bound dimer, $(CH_3)_3CO(H)(NO)^+((CH_3)_3CNO_2)$, can dissociate into *t*-butanol and $((CH_3)_3CNO_2)(NO)^+$ with a dissociation energy of 90 kJ mol^{-1} (calculated at B3-LYP/6-31 + G(d)). It has previously been shown that B3-LYP gives an erroneous energy for NO^+ [40]. So, G3 calculations were performed on both these dissociation products and the products $(CH_3)_3CNO_2H^+ + (CH_3)_3CNO_2$ for comparison. The G3 calculations result in a relative dissociation energy for the two sets of products that is 9 kJ mol^{-1} lower than the B3-LYP results, indicating that B3-LYP is treating $((CH_3)_3CNO_2)(NO)^+$ in a reasonable fashion.

3. Results and discussion

3.1. Mass spectrometric studies of $(RNO_2)_2H^+$

Metastable ion (MI) mass spectrometry probes the accessible reaction channels that occur spontaneously without the aid of collisions. Our MI experiments on a series of $(RNO_2)_2H^+$ where R = CH_3, CH_2CH_3, $(CH_3)_2CH$ and $(CH_3)_3C$ reflect how the methyl groups on the nitroalkane affect the competition of the reaction channels on the microsecond timescale.

The MI mass spectra of these four methyl-substituted proton-bound dimers are presented in Fig. 1a. They all exhibit a peak nominally due to the protonated nitroalkane. In the cases of $(CH_3NO_2)_2H^+$ and $(CH_3CH_2NO_2)_2H^+$, this reaction is the only reaction channel observed on the microsecond timescale.

The MI mass spectra of $((CH_3)_2CHNO_2)_2H^+$ and $((CH_3)_3CNO_2)_2H^+$ exhibit a second channel that leads to the loss of 47 Da that can only be attributed to the loss of nitrous acid

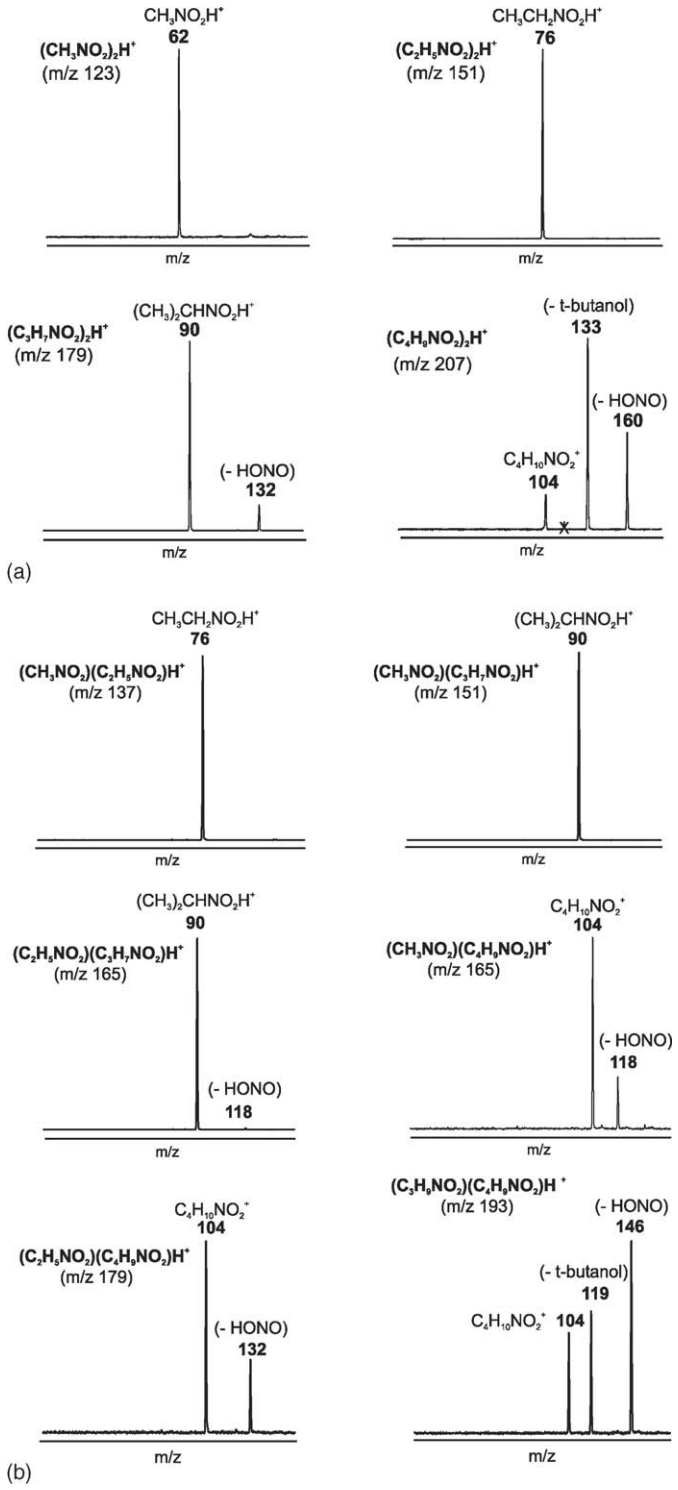

Fig. 1. (a) MI mass spectra of the proton-bound dimers $(CH_3NO_2)_2H^+$, $(CH_3CH_2NO_2)_2H^+$, $((CH_3)_2CHNO_2)_2H^+$ and $((CH_3)_3CNO_2)_2H^+$. (b) MI mass spectra of the unsymmetric proton-bound pairs. The mark "X" indicates an artifact peak that results from an impurity in the ion beam.

(HONO). The similarity between these proton-bound dimers and those previously studied [17–19] suggests that the loss of nitrous acid is likely to be the result of an S_N2-type of rearrangement (Scheme 1). Deuterium-labelling of the bridging proton in $((CH_3)_3CNO_2)_2H^+$ confirms that the nitrous acid loss involves the bridging proton and that there is no hydrogen exchange between this proton and the alkyl hydrogens. The MI results also indicate that methyl substituents favour this rearrangement process, similar to that observed for $(ROH)(R'OH)H^+$ and $(RCN)(R'OH)H^+$ [18].

The MI mass spectrum of $((CH_3)_3CNO_2)H^+$ exhibits a third channel, the loss of 74 Da. The resulting ion (*m/z* 133) was transmitted to the third field-free region where it was analyzed by collision-induced dissociations (CID). The identity of this ion is discussed separately below.

3.2. Mass spectrometric studies of $(R_1NO_2)(R_2NO_2)H^+$

Unsymmetric proton-bound pairs have also been investigated. Their MI mass spectra are presented in Fig. 1b. All cases exhibit the formation of protonated nitroalkane. Nitrous acid loss was observed from $(CH_3NO_2)((CH_3)_3CNO_2)H^+$, $(CH_3CH_2NO_2)((CH_3)_2CHNO_2)H^+$, $(CH_3CH_2NO_2)((CH_3)_3CNO_2)H^+$ and $((CH_3)_2CHNO_2)((CH_3)_3CNO_2)H^+$, emphasizing the importance of highly methyl-substituted species in the proton-bound pair in favouring the rearrangement. This observation also indicates that in $(CH_3CH_2NO_2)((CH_3)_2CHNO_2)H^+$, $(CH_3NO_2)((CH_3)_3CNO_2)H^+$ and $(CH_3CH_2NO_2)((CH_3)_3CNO_2)H^+$, the reaction proceeds exclusively through isopropyl or *t*-butyl transfer as methyl and ethyl transfer do not occur. The *t*-butanol loss channel is observed for $((CH_3)_2CHNO_2)((CH_3)_3CNO_2)H^+$ only, confirming the important role the *t*-butyl substituent plays in this process. MI experiments with the deuterium-labelled species $((CD_3)_2CHNO_2)((CH_3)_3CNO_2)D^+$ and $((CD_3)_2CHNO_2)((CH_3)_3CNO_2)H^+$ excludes the involvement of the $(CH_3)_2CH$ moiety in the neutral product. The nature of this *m/z* 119 ion is discussed below.

3.3. The identity of m/z 119 and 133

The metastably generated *m/z* 119 ion (from $((CH_3)_2CHNO_2)((CH_3)_3CNO_2)H^+$) was transmitted to the third field-free region where it was analyzed by CID. The CID mass spectrum shows intense peaks at *m/z* 30 (NO^+) and 43 ($(CH_3)_2CH^+$) as well as several smaller peaks (see Fig. 2a). To test that this ion was due to the interaction of NO^+ and $(CH_3)_2CHNO_2$, NO and $(CH_3)_2CHNO_2$ were co-introduced into the ion source and the resulting ion at *m/z* 119 (having 5 kV translational energy) was transmitted to the second field-free region. The CID mass spectrum (Fig. 2b) of this ion is similar to Fig. 2a, confirming that the product ion (*m/z* 119) derived from $((CH_3)_2CHNO_2)((CH_3)_3CNO_2)H^+$ to be a complex between NO^+ and $(CH_3)_2CHNO_2$. There are some variations in the relative intensities of the peaks, especially those of the weaker ones. This is subject to the reproducibility of the spectrum due to the weak signal that was being transmitted to the third field-free region. Further supporting the nature of this structure is the MI mass spectrum of the source-generated complex which gives a sharp peak at *m/z* 30 and a much smaller peak at *m/z* 72 (relative intensity ratio of 30: 72 is 1.0: 0.04). The observation of NO^+ instead of $(CH_3)_2CHNO_2{}^+$ agrees with the relative ionization energies of NO and 2-nitropropane

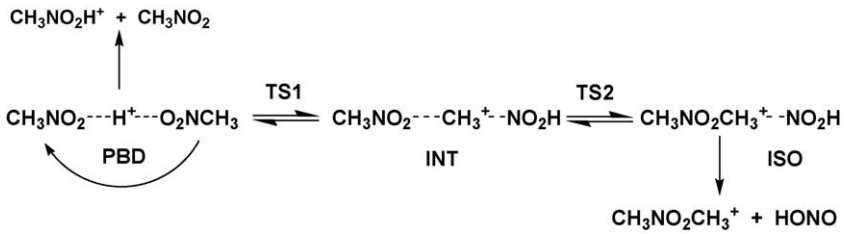

Scheme 1.

(9.26 and 10.74 eV respectively) [41]. The NR mass spectrum of the source-generated complex (Fig. 2c) exhibits three main peaks, *m/z* 30, 43 and 46. The precursor ion (*m/z* 119) can either be neutralized upon collision in the first collision cell or dissociate to give $NO^+ + (CH_3)_2CHNO_2$. The resulting neutral $(CH_3)_2CHNO_2$ can then be reionized to form $(CH_3)_2CHNO_2^+$, which falls apart into the isopropyl cation (*m/z* 43) and NO_2 due to the low stability of the ion (for example, the molecular ion is barely observed in the EI mass spectrum of 2-nitropropane [41].) The ions at *m/z* 30 and 46 arise from the dissociation of the *m/z* 119 into the isopropyl cation and neutral NO_2 and NO (which could be a complex) which are then reionized into NO_2^+ and NO^+. All of these experiments suggest a structure for the *m/z* 119 ion in which NO^+ is electrostatically bound to $(CH_3)_2CHNO_2$.

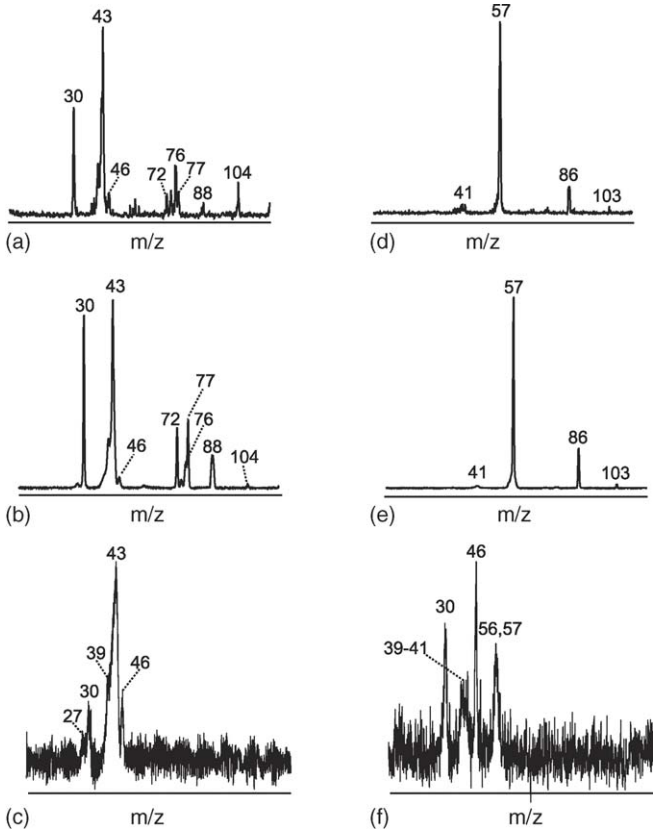

Fig. 2. CID mass spectra of (a) metastably-generated *m/z* 119 from the proton-bound pair $((CH_3)_2CHNO_2)((CH_3)_3CNO_2)H^+$ and (b) source-generated *m/z* 119 $((CH_3)_2CHNO_2)(NO)^+$ at 5 kV. (c) NR mass spectrum of source-generated *m/z* 119 $((CH_3)_2CHNO_2)(NO)^+$ at 5 kV. CID mass spectra of (d) metastably-generated *m/z* 133 from the proton-bound dimer $((CH_3)_3CNO_2)_2H^+$ and (e) source-generated *m/z* 133 $((CH_3)_3CNO_2)(NO)^+$ at 5 kV. (f) NR mass spectrum of source-generated *m/z* 133 $((CH_3)_3CNO_2)(NO)^+$ at 5 kV. The labels 39–41 and 56, 57 indicate relatively broad peaks that cover more than one mass.

The fragment ion having *m/z* 133 from $((CH_3)_3CNO_2)_2H^+$ was transmitted to the third field-free region where it was analyzed by CID. The CID mass spectrum shows intense peaks at *m/z* 57 ($(CH_3)_3C^+$) and 86 ($C_4H_8NO^+$) (see Fig. 2d). This spectrum is similar to the CID mass spectrum of the ion generated from the association reaction of NO^+ and $(CH_3)_3CNO_2$ in the ion source (Fig. 2e). These two peaks are also observed in the MI mass spectrum except that the peak at *m/z* 86 (due to loss of HONO, obviously resulting from a rearrangement) is more intense than *m/z* 57. Strikingly, no NO^+ was observed in any of these spectra. Based on the ionization energies of NO and 2-methyl-2-nitropropane (9.26 [41] and 10.47 eV respectively, the latter being calculated at the G3 level of theory), formation of NO^+ might be expected to be the favoured product. G3 calculations based on B3-LYP geometries found the lowest energy dissociation products to be $(CH_3)_3C^+ + N_2O_3$, which lie 8 kJ/mol lower than $(CH_3)_3CNO_2 + NO^+$. Therefore, the stability of the *t*-butyl ion has favoured the dissociation forming the *t*-butyl cation over that which makes NO^+. As NO^+ was not observed in the MI mass spectrum, the nature of how NO^+ is bound to the molecule cannot be determined. The NR mass spectrum of the source-generated complex (Fig. 2c) exhibits several peaks. The *m/z* 133 ions neutralized in the first collision cell would likely fall apart into NO and 2-methyl-2-nitropropane. Upon reionization, ionized 2-methyl-2-nitropropane would itself dissociate into the *t*-butyl cation (*m/z* 57) and NO_2 due to the low stability of the molecular ion (the molecular ion is not observed in the EI mass spectrum of 2-methyl-2-nitropropane [41]). The peak with *m/z* 46 can arise from the dissociation in the first collision cell of the *m/z* 133 ion into the *t*-butyl cation and N_2O_3 (or $NO_2 + NO$) which is then reionized to NO_2^+ (*m/z* 46) and NO^+ (*m/z* 30). Based on G3 calculations on B3-LYP geometries, N_2O_3 is very weakly bound with respect to $NO_2 + NO$ (N–N bond = 1.9 Å and binding energy = 37 kJ mol^{-1}). $N_2O_3^+$ was not observed in the NR mass spectrum due to the instability of the ion. G3 calculations give an N–N bond length of 2.5 Å and a binding energy of −11 kJ mol^{-1} with respect to $NO^+ + NO_2$ for $N_2O_3^+$. While it is hard to believe that there is no binding energy when NO^+ interacts with NO_2, the calculations indicate that this binding will be small. These experimental and theoretical results are at least consistent with an electrostatically bound complex structure $((CH_3)_3CNO_2)(NO^+)$ for *m/z* 133.

3.4. Nitro-nitrite rearrangement and the alcohol loss channel

The most reasonable mechanism for the formation of neutral *t*-butanol is one in which there is a nitro-nitrite rearrangement leading to a nitrite isomer that can then lose *t*-butanol (74 Da). A similar loss of *t*-butanol from the associative ion–molecule reactions of *t*-butyl nitrite with enol ions [42] or protonated aromatics [43] further supports the proposed mechanism. It is worth noting that the rearrangement turns out to be the kinetically most favoured channel on the microsecond timescale for $((CH_3)_3CNO_2)_2H^+$ but no loss of any other alcohol was observed from the other proton-bound dimers, emphasizing the importance of the *t*-butyl substituent in favouring this rearrangement process.

The observation of a nitro-nitrite rearrangement in $((CH_3)_3CNO_2)_2H^+$ led to an investigation of the effect of protonation on the process in isolated nitroalkanes. Is the barrier significantly lowered when a species is protonated, as was found for the case of radical cations [31]? If so, this rearrangement may be significant in the ion source of the mass spectrometer and hence influence the nature of the proton-bound pairs generated therein.

The nitro-nitrite rearrangement of nitromethane is slightly endothermic ($\Delta E = 11$ kJ mol^{-1}) with a high activation barrier (272 kJ mol^{-1}) (Fig. 3a) This value is in fairly good agreement with values from QCISD/6-31G(d), MP2/6-31G(d) and MP2/6-311++G(df,p) levels of theory, though the energy can range from 244 to 357 kJ mol^{-1}, depending on the level of theory [31]. IRC calculations clearly show that this reaction path leads to the

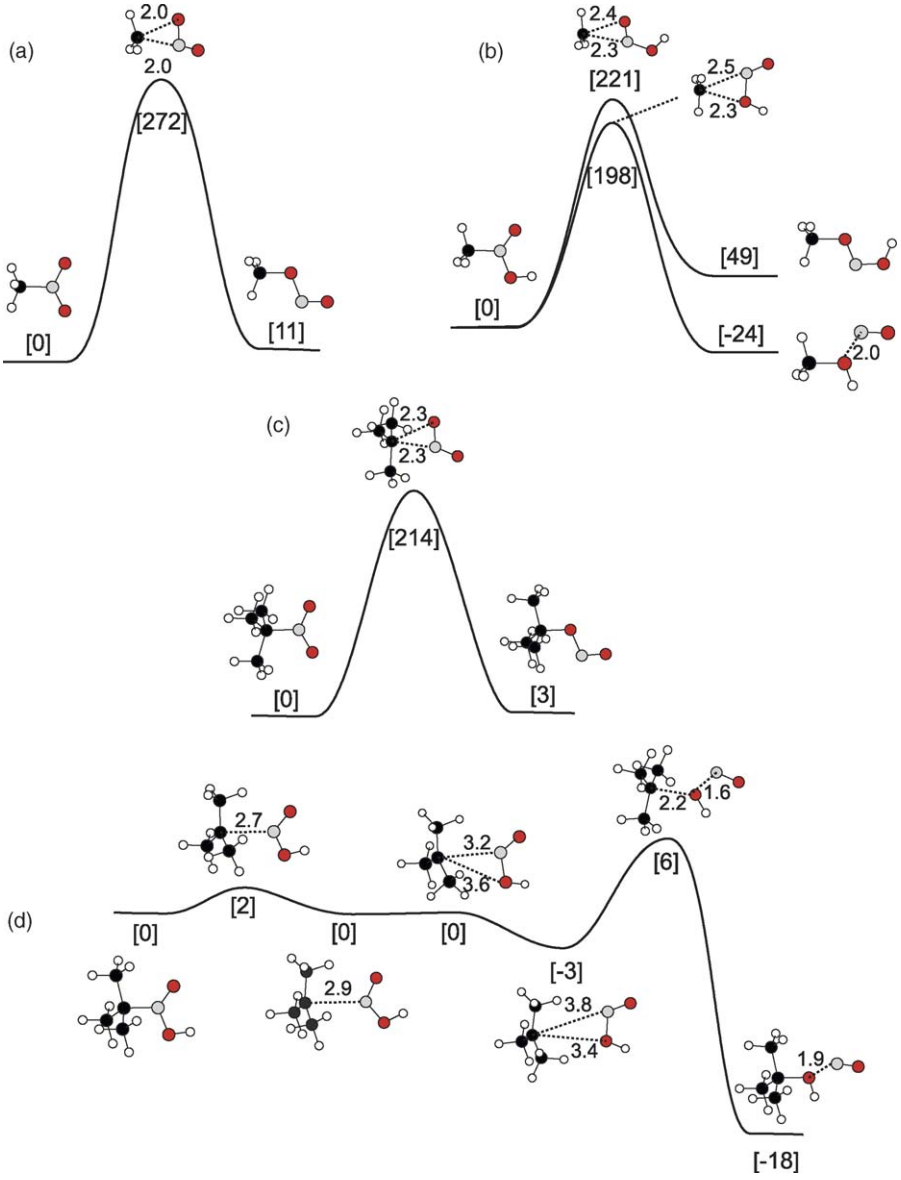

Fig. 3. Potential energy surface with relative energies (in square brackets, kJ mol^{-1}) and corresponding geometries for the nitro-nitrite rearrangement of (a) CH_3NO_2, (b) $CH_3NO_2H^+$, (c) $(CH_3)_3CNO_2$ and (d) $(CH_3)_3CNO_2H^+$ calculated at the B3-LYP/6-31 + G(d) level of theory. Bond length values are in angstroms. The trans isomer of the protonated nitrite products lie 1–4 kJ mol^{-1} lower in energy.

trans-isomer and confirm the concerted behaviour of the transition state noted by Arenas et al. [29].

The nitro-nitrite rearrangement of protonated nitromethane consists of two distinct pathways (Fig. 3b). The methyl group can migrate to either oxygen to form both *cis*-and *trans*-isomers with respect to the proton. Transfer to the protonated oxygen is more favourable (lower by about 23 kJ mol^{-1}), driven by the exothermicity of the process. The product of this isomerization may also be described as a complex of NO^+ and methanol separated by 2.0 Å. Compared to its neutral form, protonation of nitromethane lowers the nitro-nitrite barrier by over 50 kJ mol^{-1}.

Results for 2-methyl-2-nitropropane and its protonated form are also compared. The mechanism for 2-methyl-2-nitropropane (Fig. 3c) is very similar to that of nitromethane and also forms a trans-isomer. The process is nearly thermoneutral with a lower barrier (214 kJ mol^{-1}) due to stabilization of the transition state by the methyl groups. The concerted motion of the transition state is also confirmed by IRC calculations. Protonating 2-methyl-2-nitropropane results in a significantly different mechanism (Fig. 3d). The rearrangement can now be described as a three-step process with "loose" transition states. The process begins by breaking the C–N bond, followed by the migration of the *t*-butyl moiety towards the oxygen atom, and finally forming a C–O bond to produce a product ion that resembles a complex between NO^+ and *t*-butanol. This multi-step process results in a nearly barrierless isomerization. So, protonated 2-methyl-2-nitropropane does not really exist as a distinct entity in the gas phase. This raises questions about the nature of the proton-bound pairs involving 2-methyl-2-nitropropane formed in the ion source of our instrument.

The potential energy surface for the nitro-nitrite isomerization for the proton-bound dimer of 2-methyl-2-nitropropane, $((CH_3)_3CNO_2)_2H^+$, is shown in Fig. 4a. The corresponding structures can be found in Fig. 5. The isomerization in the proton-bound dimer **4**–**14** follows a multi-step mechanism similar to that of isolated protonated 2-methyl-2-nitropropane as in Fig. 3d. The nitrite form **14** is only 8 kJ mol^{-1} higher in energy than the proton-bound dimer but the intermediate **13** is raised by 57 kJ mol^{-1} compared to that shown in Fig. 3d. The transition states were not found for this process due to the difficulty in calculating such large molecules. It is reasonable to believe that these barriers are not very large as optimization jobs of slightly modified geometries of the intermediate fall into the two deeper potential energy wells. We can conclude therefore that the initially formed proton-bound complex can be a mixture of **4** $((CH_3)_3CNO_2)_2H^+$ and **14** $(CH_3)_3CO(H)(NO)^+((CH_3)_3CNO_2)$ which will interconvert below their dissociation limits.

In addition, *t*-butanol loss could also result from a nitro-nitrite rearrangement in structure **8** in Figs. 4a, 5. Isomers of **8** that consist of $(CH_3)_3CNO_2\cdots(CH_3)_3C\cdots NO_2H^+$ are calculated to have relative energies of 61, 60 and 63 kJ/mol for **16**, **17** and **18**, respectively. Assuming a small barrier between **8** and these isomers (see Fig. 3d), **8** could also act as a precursor to *m/z* 133.

The total potential energy surface for $((CH_3)_3CNO_2)_2H^+$ is presented in Fig. 4b. The nitrite form of the proton-bound pair **14** can also dissociate into protonated *t*-butyl nitrite and neutral 2-methyl-2-nitropropane by a simple hydrogen-bond cleavage

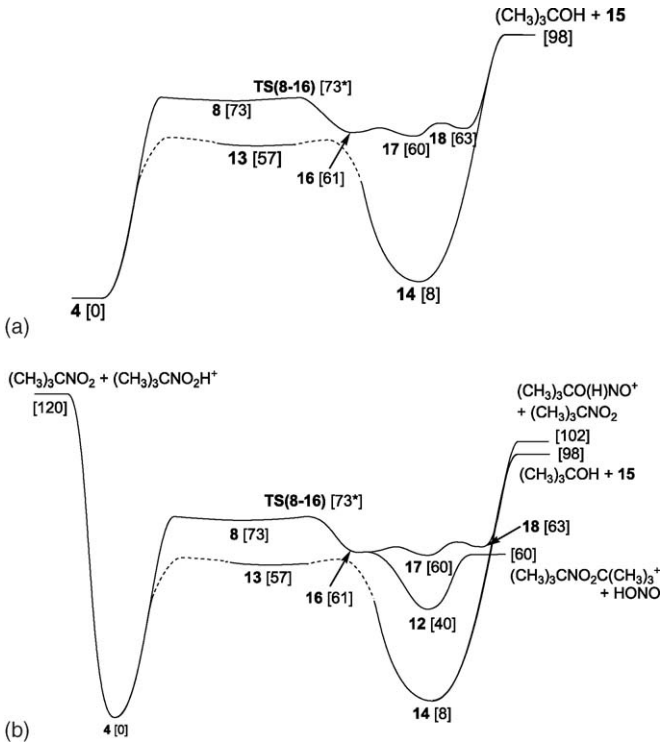

Fig. 4. (a) Potential energy surface (with relative energies in square brackets, kJ mol^{-1}) for the loss of *t*-butanol from the proton-bound dimer $[(CH_3)_3CNO_2]_2H^+$, (b) Complete potential energy surface for $[(CH_3)_3CNO_2]_2H^+$. Calculations were performed at B3-LYP/6-31 + G(d) level of theory. The value marked with × comes from an opt = qst2 calculation in Gaussian 98. Structures are shown in Fig. 5.

(Fig. 4b). This dissociation energy lies about 4 kJ mol^{-1} higher than that leading to the loss of *t*-butanol at the B3-LYP/6-31 + G(d) level of theory. The dissociation channel producing protonated *t*-butyl nitrite could therefore compete with the loss of *t*-butanol. In contrast, the dissociation of the proton-bound 2-methyl-2-nitropropane dimer **4** into protonated and neutral 2-methyl-2-nitropropane requires an energy of 120 kJ mol^{-1}. Both dissociation channels are probably accessible but *m/z* 104 in Fig. 1a is likely to be coming primarily from the nitrite isomer. In addition, since there is only a 6 kJ mol^{-1} barrier between protonated 2-methyl-2-nitropropane and protonated *t*-butyl nitrite (Fig. 3d), the fragment ion at *m/z* 104 will be a mixture of the two species, and it would be impossible to characterize them individually.

3.5. Nitrous acid loss channel

The theoretical reaction profile for $(CH_3NO_2)_2H^+$ at the B3-LYP/6-31 + G(d), MP2/6-31 + G(d) and G3 levels of theory are presented in Fig. 6 (corresponding structures are shown in Fig. 5). The isomerization reaction resulting in HONO loss involves an S_N2-type of mechanism. The first step of the process consists of a barrier (**TS(1–5)**, TS1) involving the rotation of one moiety where the neutral nitroalkane migrates to set up for a backside attack on the protonated species. This barrier is small (almost negligible) relative to the intermediate (**5**, INT). The sec-

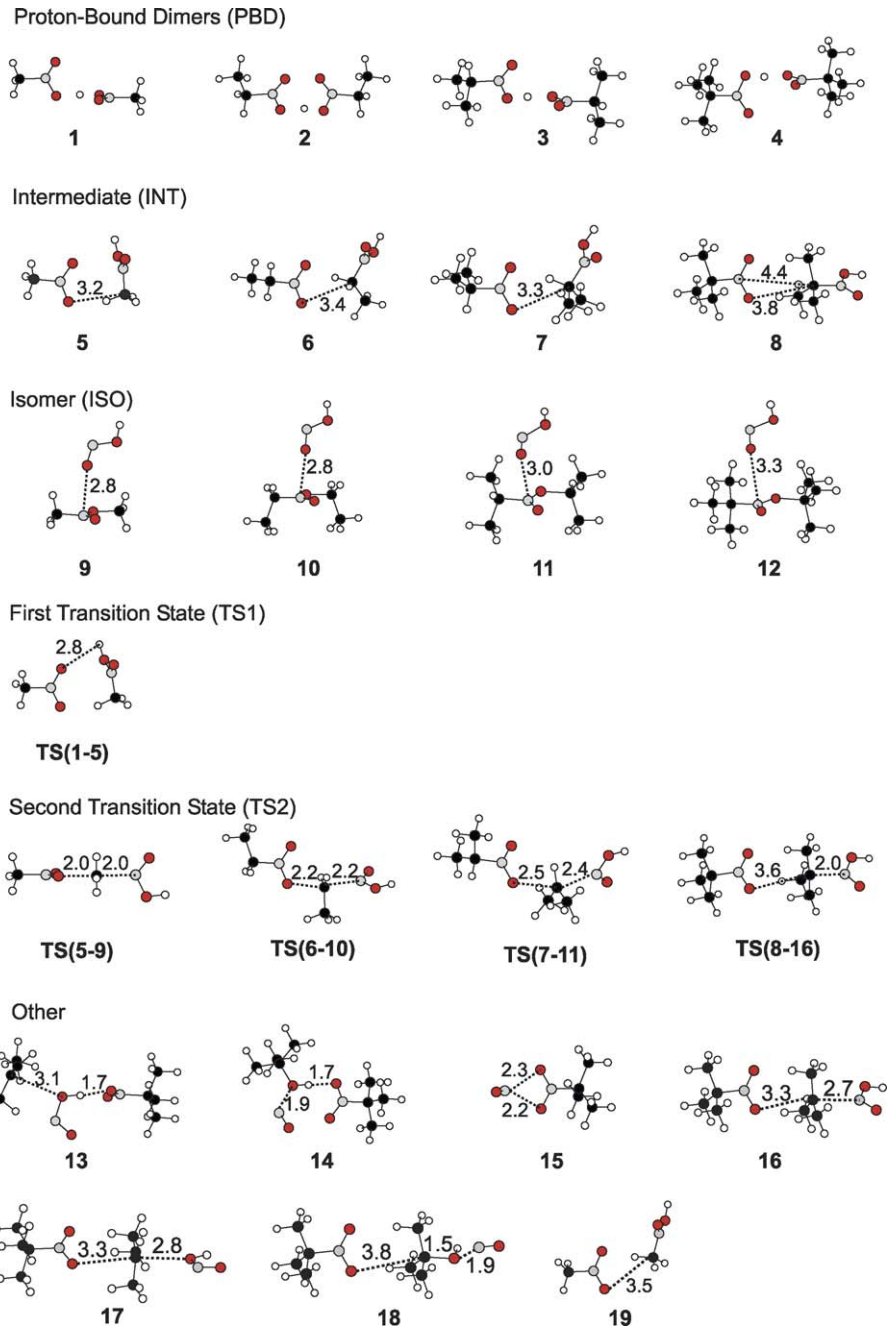

Fig. 5. Optimized geometries at the B3-LYP/6-31 + G(d) level of theory. Selected bond length values are presented in angstroms.

ond step (the key barrier in the rearrangement, TS2, see **TS(5–9)** in Fig. 5) involves an alkyl cation transfer, where the attack of the neutral molecule on the carbon results in the lengthening of the C–N bond in the protonated nitromethane moiety and the shortening of the O–C bond in $[CH_3NO_2\cdots CH_3\cdots NO_2H]^{+\ddagger}$. After some conformational changes, it results in a thermodynamically stable isomer **9**, $(HONO)(CH_3NO_2CH_3)^+$. Simple dissociation from this complex results in the final products of $CH_3NO_2CH_3^+$ and HONO. Another conformer of **5** was found to lie 10 kJ/mol higher in energy (see **19** in Fig. 5) which may be involved in the conversion of **5** to **TS(5–9)**.

Three isomeric structures of nitrous acid were calculated: HNO_2, where the hydrogen is bonded to the nitrogen and *cis*-and *trans*-HONO. HONO has been a subject of extensive theoretical and experimental investigations [44]. The trans conformer of HONO is the most stable structure lying 1 kJ mol^{-1} lower than the cis conformer and 24 kJ mol^{-1} below HNO_2. The final product of the isomerization process should therefore be a mixture of *trans*-and *cis*-HONO.

The effect of the HONO conformation in the transition state was also examined. Calculations show that TS(5–9) in which the proton is in the cis conformation lies 19 kJ mol^{-1} below its

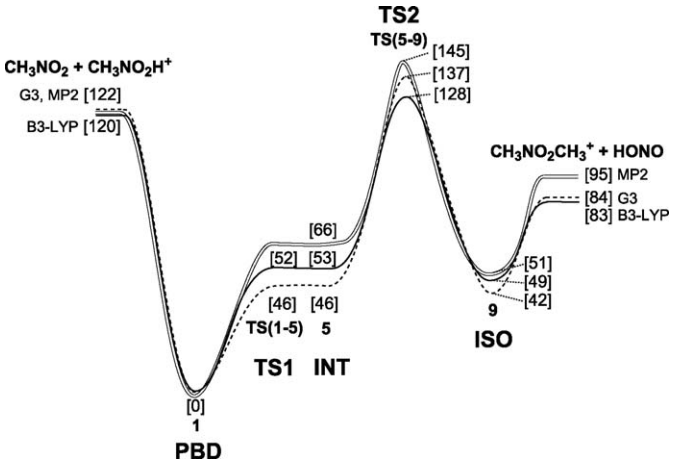

Fig. 6. Potential energy surface for the isomerization of the nitromethane proton-bound dimer $(CH_3NO_2)_2H^+$ leading to loss of nitrous acid, calculated at the B3-LYP/6-31 + G(d) (–), MP2/6-31 + G(d) (==) and G3 (—) levels of theory. Relative energy values (kJ mol^{-1}) for MP2, G3 and B3-LYP are in square brackets. Optimized geometries at B3-LYP/6-31 + G(d) level of theory are presented in Fig. 5.

trans conformer; the *cis–trans* conformational change in HONO should thus occur primarily after the alkyl cation transfer step is completed.

The surface for this S_N2-type rearrangement in $(CH_3NO_2)_2H^+$ was also calculated at the MP2/6-31 + G(d) and G3 (on B3-LYP geometries) levels of theory (Fig. 6). The G3 value for TS2 lies between the B3-LYP and MP2 results. In general, there is consistency between the three levels of theory.

The relative energies of the dissociation and S_N2-isomerization process for the other symmetric nitroalkane proton-bound dimers are included in Figs. 7, 4b for comparison. The threshold to dissociation to protonated and neutral nitroalkane does not vary significantly with methyl substitution, ranging from 120 to 125 kJ mol^{-1}. This is consistent with the trends observed for other symmetric proton-bound pairs [45]. The isomerization barrier is consistently decreased

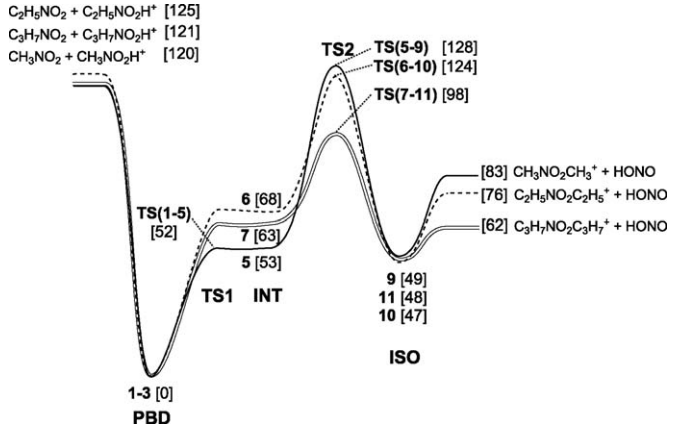

Fig. 7. Potential energy surface with relative energies (in square brackets, kJ mol^{-1}) for the proton-bound dimer of nitromethane (–), nitroethane (—) and 2-nitropropane (==) to lose nitrous acid at the B3-LYP/6-31 + G(d) level of theory. Optimized geometries are presented in Fig. 5.

with increased methyl substitution, going from 128 kJ mol^{-1} for $(CH_3NO_2)_2H^+$, to 124 kJ mol^{-1} for $(CH_3CH_2NO_2)_2H^+$ and 98 kJ mol^{-1} for $((CH_3)_2CHNO_2)_2H^+$, a result of charge stabilization in TS2. The fact that the isomerization and dissociation thresholds are similar for $(CH_3NO_2)_2H^+$ and $(CH_3CH_2NO_2)_2H^+$ and yet no nitrous acid loss is observed is a clear indication of the less favourable entropies for the former process [46]. The tighter transition state associated with the S_N2 rearrangement reduces the rate constant of the process in comparison to the simple H-bond cleavage reaction, resulting in the former being non-competitive with the latter.

The theoretical reaction profile of $((CH_3)_3CNO_2)_2H^+$ is presented in Fig. 4b. The rearrangement barrier (**TS(8–16)**, TS2) is decreased substantially compared to that of the other nitroalkane proton-bound pairs, in good agreement with the experimental result. However, the barrier is lowered to an extent that the rearrangement process evolves over a rather flat surface, with the alkyl cation transfer barrier TS2 lying close in energy to the barrier (TS1) for forming the intermediate (**8**, INT) from the original proton-bound dimer **4**. In addition, the alkyl cation transfer (TS2) has also changed from a one-step to a two-step process. A stable minimum structure (**16** in Figs. 4b, 5) was found at the mid-way point of the alkyl cation transfer step. This result reflects the increased stability of the *t*-butyl ion in the gas phase.

It is conceivable that a 1,5-hydrogen shift in the product ion $(RNO_2R'^+)$ could result in the formation of a protonated nitroalkane (RNO_2H^+) and a neutral alkene. Based on their heats of formation [41] the products $(CH_3)_3CNO_2H^+ + CH_2C(CH_3)_2 +$ HONO lie 80 kJ mol^{-1} above $(CH_3)_3CNO_2H^+ + (CH_3)_3CNO_2$ and thus 140 kJ mol^{-1} above $(CH_3)_3CNO_2H^+ +$ HONO, and will not be accessible to the metastable ions in this study.

4. Conclusions

The unimolecular chemistry of a series of nitroalkane proton-bound pairs was investigated. This chemistry can involve hydrogen-bond cleavage reactions, an internal S_N2-type reaction that leads to loss of HONO and, for the pairs involving 2-methyl-2-nitropropane, a nitro-nitrite rearrangement that leads to the loss of *t*-butanol. The loss of nitrous acid is the result of an internal S_N2 rearrangement that involves the formation of intermediate complexes ($RNO_2\cdots R'NO_2H^+$ and $RNO_2R'^+\cdots$HONO) prior to the loss of HONO. This rearrangement is favoured by methyl substitution and actually becomes more of an S_N1-type mechanism when 2-methyl-2-nitropropane is involved. The unimolecular chemistry of the proton-bound pairs involving 2-methyl-2-nitropropane is also affected by a low isomerization barrier between protonated 2-methyl-2-nitropropane and protonated *t*-butyl nitrite. This results in a mixture of nitro–nitro and nitro–nitrite proton-bound pairs in the ion source. Addition of a neutral nitroalkane to the protonated species (to make a proton-bound pair) raises the interconversion barrier between the nitro and nitrite alkanes, but does not prevent their interconversion. The nitrite isomer of the proton-bound pair can dissociate by loss of *t*-butanol to form an ionic complex between a nitroalkane and NO^+.

Acknowledgements

PMM thanks the Natural Sciences and Engineering Research Council (NSERC) of Canada for continuing financial support. CP thanks NSERC for a postgraduate scholarship during the tenure of which this work is completed.

Appendix A. Supplementary data

Supplementary data associated with this article can be found, in the online version, at doi:10.1016/j.ijms.2006.01.036.

References

[1] J.L. Beauchamp, M.C. Caserio, J. Am. Chem. Soc. 94 (1972) 2638.
[2] J.L. Beauchamp, M.C. Caserio, T.B. McMahon, J. Am. Chem. Soc. 96 (1974) 6243.
[3] F. Mafune, J. Kohno, T. Kondow, J. Phys. Chem. 100 (1996) 10041.
[4] X. Zhang, X. Yang, A.W. Castleman, Chem. Phys. Lett. 185 (1991) 298.
[5] W.Y. Feng, C. Lifshitz, Int. J. Mass Spectrom. Ion Processes 149/150 (1995) 13.
[6] G. Bouchoux, N. Choret, Rapid Commun. Mass Spectrom. 11 (1997) 1799.
[7] K. Raghavachari, J. Chandrasekhar, R.C. Burnier, J. Am. Chem. Soc. 106 (1984) 3124.
[8] J.C. Sheldon, G.J. Currie, J.H. Bowie, J. Chem. Soc. Perkin Trans. 27 (1986) 941.
[9] G.D. Ruggiero, I.H. Williams, J. Chem. Soc. Perkin Trans. 22 (2002) 591.
[10] T.D. Fridgen, T.B. McMahon, J. Phys. Chem. A 107 (2003) 668.
[11] T.D. Fridgen, T.B. McMahon, J. Phys. Chem. A 106 (2002) 9648.
[12] Z. Karpas, M. Meot-Ner, J. Phys. Chem. 93 (1989) 1859.
[13] H.E. Audier, C. Monteiro, P. Mourgues, D. Robin, Rapid Commun. Mass Spectrom. 3 (1989) 84.
[14] J.C. Kleingeld, N.M.M. Nibbering, Org. Mass Spectrom. 17 (1982) 136.
[15] S.T. Graul, R.R. Squires, Int. J. Mass Spectrom. Ion Processes 81 (1987) 183.
[16] T.T. Dang, V.M. Bierbaum, Int. J. Mass Spectrom. Ion Processes 117 (1992) 65.
[17] R.A. Ochran, A. Annamalai, P.M. Mayer, J. Phys. Chem. A 104 (2000) 8505.
[18] R.A. Ochran, P.M. Mayer, Eur. Mass Spectrom. 7 (2001) 267.
[19] J. Grabowy, P.M. Mayer, Can. J. Chem. 83 (2005) 1864.
[20] T.D. Fridgen, J.D. Keller, T.B. McMahon, J. Phys. Chem. A 105 (2001) 3816.
[21] T.D. Fridgen, T.B. McMahon, J. Am. Chem. Soc. 123 (2001) 3980.
[22] A.M. Wodtke, E.J. Hintsa, Y.T. Lee, J. Phys. Chem. 90 (1986) 3549.
[23] A.M. Wodtke, E.J. Hintsa, Y.T. Lee, J. Chem. Phys. 84 (1986) 1044.
[24] M.J.S. Dewar, J.P. Ritchie, J. Org. Chem. 50 (1985) 1031.
[25] M.L. McKee, J. Am. Chem. Soc. 108 (1986) 5784.
[26] M.L. McKee, J. Phys. Chem. 93 (1989) 7365.
[27] R.P. Saxon, M. Yoshimine, Can. J. Chem. 70 (1992) 572.
[28] M.R. Manaa, L.E. Fried, J. Phys. Chem. A 102 (1998) 9884.
[29] J.F. Arenas, S.P. Centeno, I. López-Tocón, D. Peláez, J. Soto, Thermochem. 630 (2003) 17.
[30] T.J. Packwood, M. Page, Chem. Phys. Lett. 216 (1993) 180.
[31] G.M. Khrapkovskii, E.V. Nikolaeva, D.V. Chachkov, A.G. Shamov, Russ. J. Gen. Chem. 74 (2004) 908.
[32] J.L. Holmes, P.M. Mayer, J. Phys. Chem. 99 (1995) 1366.
[33] E.E. Rennie, P.M. Mayer, J. Chem. Phys. 120 (2004) 10561.
[34] K.L. Busch, G.L. Glish, S.A. McLuckey, Mass Spectrometry/Mass Spectrometry, VCH Publishers, New York, 1988.
[35] J.C. Traeger, A.A. Mommers, Org. Mass Spectrom. 22 (1987) 592.
[36] W.J. Hehre, L. Radom, P.v.R. Schleyer, J.A. Pople, Ab Initio Molecular Orbital Theory, Wiley, New York, 1986.
[37] M.J. Frisch, G.W. Trucks, H.B. Schlegel, G.E. Scuseria, M.A. Robb, J.R. Cheeseman, V.G. Zakrzewski, J.A. Montgomery, R.E. Stratmann, J.C. Burant, S. Dapprich, J.M. Millam, A.D. Daniels, K.N. Kudin, M.C. Strain, O. Farkas, J. Tomasi, V. Barone, M. Cossi, R. Cammi, B. Mennucci, C. Pomelli, C. Adamo, S. Clifford, J. Ochterski, G.A. Petersson, P.Y. Ayala, Q. Cui, K. Morokuma, D.K. Malick, A.D. Rabuck, K. Raghavachari, J.B. Foresman, J. Cioslowski, J.V. Ortiz, B.B. Stefanov, G. Liu, A. Liashenko, P. Piskorz, I. Komaromi, R. Gomperts, R.L. Martin, D.J. Fox, T. Keith, M.A. Al-Laham, C.Y. Peng, A. Nanayakkara, C. Gonzalez, M. Challacombe, P.M.W. Gill, B. Johnson, W. Chen, M.W. Wong, J.L. Andres, C. Gonzalez, M. Head-Gordon, E.S. Replogle, J.A. Pople. 1998. GAUSSIAN 98 Rev. A.6. In: GAUSSIAN., 98, Rev., A.6., Pittsburgh PA: Gaussian, Inc.
[38] A.P. Scott, L. Radom, J. Phys. Chem. 100 (1996) 16502.
[39] A.G. Baboul, L.A. Curtiss, P.C. Redfern, J. Chem. Phys. 110 (1999) 7650.
[40] J.A.D. Grabowy, P.M. Mayer, Eur. J. Mass Spectrom. 10 (2004) 899.
[41] P.J. Linstrom, W.G. Mallard (Eds.), NIST Chemistry WebBook, NIST Standard Reference Database Number 69, National Institute of Standards and Technology, Gaithersburg, 2005 http://webbook.nist.gov.
[42] P. Gerbaux, P. Wantier, P.C. Nam, M.T. Nguyen, G. Bouchoux, R. Flammang, Eur. J. Mass Spectrom. 10 (2004) 889.
[43] N. Dechamps, P. Gerbaux, R. Flammang, G. Bouchoux, P.-C. Nam, M.-T. Nguyen, Int. J. Mass Spectrom. 232 (2004) 31.
[44] F. Reiche, B. Abel, R.D. Beck, T.R. Rizzo, J. Chem. Phys. 112 (2000) 8885.
[45] J.W. Larson, T.B. McMahon, J. Am. Chem. Soc. 104 (1982) 6255.
[46] T. Baer, W.L. Hase, Unimolecular Reaction Dynamics: Theory and Experiments, Oxford University Press, New York, 1996.